

Weak Interaction Processes with Relativistic Energy Density Functionals

N. Paar

Department of Physics

Faculty of Science University of Zagreb, Croatia



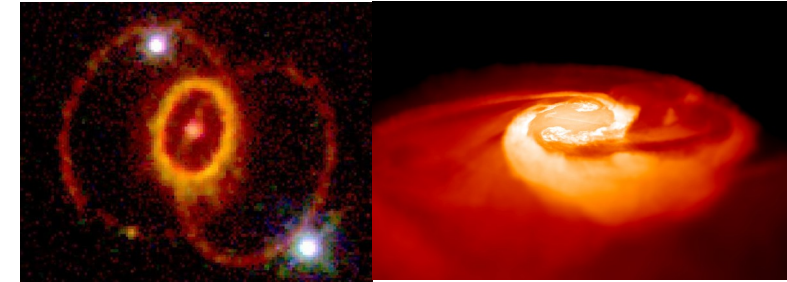
QuantiXLie

CENTER OF EXCELLENCE FOR THE THEORY OF QUANTUM AND COMPLEX SYSTEMS AND LIE ALGEBRA REPRESENTATION



INTRODUCTION

- Accurate description of nuclear properties and processes is essential for understanding the evolution of stars and nucleosynthesis (supernovae, neutron star mergers)

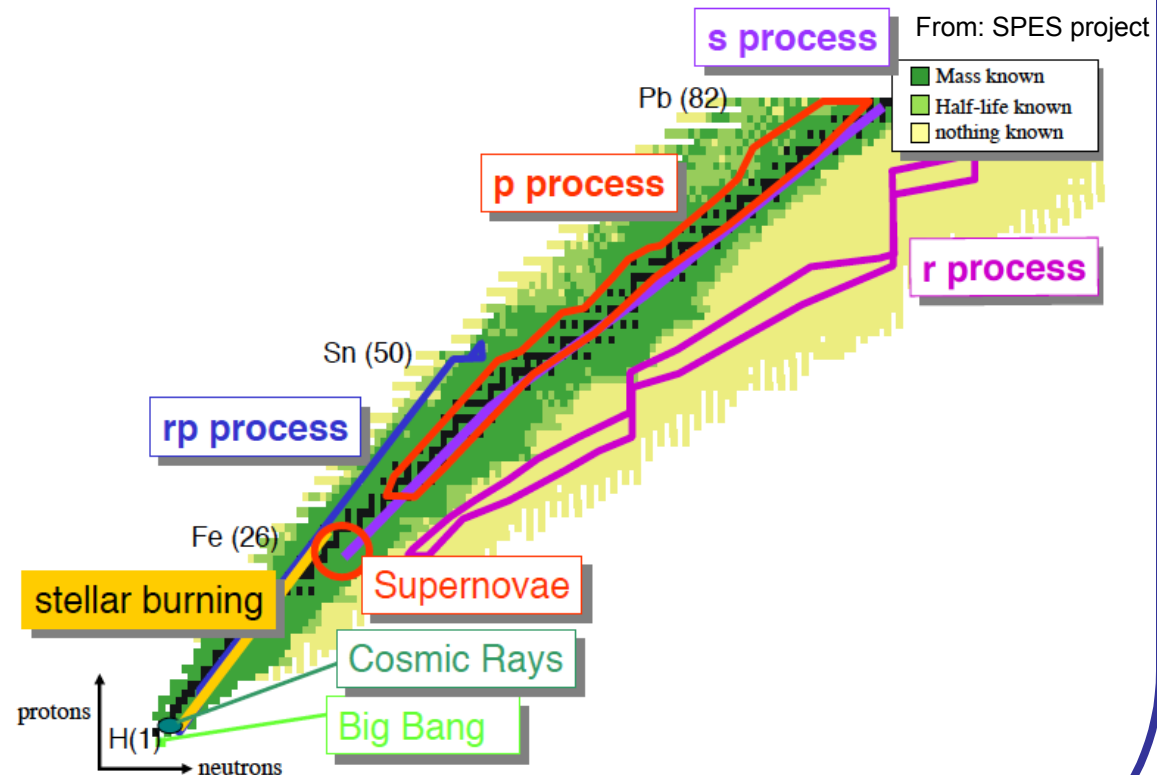


- Astrophysically relevant nuclear processes, e.g.,

- electron capture
- beta decay
- neutrino-nucleus reactions
- neutron capture
- photodissociation
- fission
- ...

- Final understanding of how supernova explosions and nucleosynthesis work, with consistent microscopic description of all relevant nuclear physics included, has not been achieved yet.

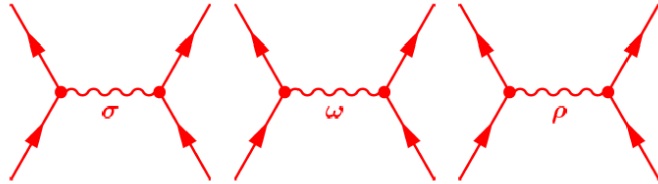
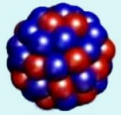
- Theoretical uncertainties in nuclear properties are mainly unknown.



RELATIVISTIC NUCLEAR ENERGY DENSITY FUNCTIONAL

i) Nucleons are Dirac particles coupled by the exchange mesons and the photon field

ii) Four-fermion contact interaction (Point-coupling model)



- Density dependent vertex functions
- The model parameters are constrained directly by many-body observables (masses, charge radii, pseudo-data, ...)
- Complicated many body dynamics encoded in the functional and its empirical constants
- DIRHB -- a relativistic self-consistent mean-field framework for atomic nuclei
Relativistic Hartree Bogoliubov model [T. Niksic et al., Comp. Phys. Comm. 185, 1808 \(2014\)](#).
- In the small amplitude limit, self-consistent relativistic quasiparticle random phase approximation (RQRPA) is used to describe excitations

ASTROPHYSICALLY RELEVANT WEAK PROCESSES

- Important weak processes during the star collapse and explosion:

$$p + e^- \rightleftharpoons n + \nu_e,$$

$$n + e^+ \rightleftharpoons p + \bar{\nu}_e,$$

$$(A, Z) + e^- \rightleftharpoons (A, Z-1) + \nu_e,$$

$$(A, Z) + e^+ \rightleftharpoons (A, Z+1) + \bar{\nu}_e,$$

$$\nu + N \rightleftharpoons \nu + N,$$

$$N + N \rightleftharpoons N + N + \nu + \bar{\nu},$$

$$\nu + (A, Z) \rightleftharpoons \nu + (A, Z),$$

$$\nu + e^\pm \rightleftharpoons \nu + e^\pm,$$

$$\nu + (A, Z) \rightleftharpoons \nu + (A, Z)^*,$$

$$e^+ + e^- \rightleftharpoons \nu + \bar{\nu},$$

$$(A, Z)^* \rightleftharpoons (A, Z) + \nu + \bar{\nu}.$$

$$\begin{aligned} \nu_l + {}_Z X_N &\rightarrow {}_{Z+1} X_{N-1}^* + l^- \\ \bar{\nu}_l + {}_Z X_N &\rightarrow {}_{Z-1} X_{N+1}^* + l^+ \end{aligned}$$

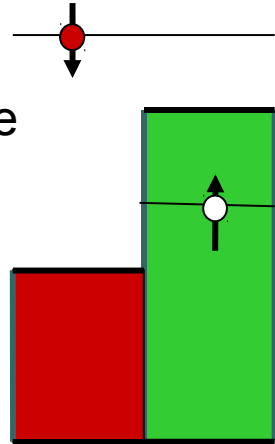


H. A. Bethe, Rev. Mod. Phys. 62 801 (1990)

K. Langanke, G. Martinez-Pinedo Rev. Mod. Phys. 75, 819 (2003)

GAMOW-TELLER TRANSITION STRENGTH FOR ^{56}Fe

Charge-exchange transitions:
e.g. spin-flip
isospin-flip



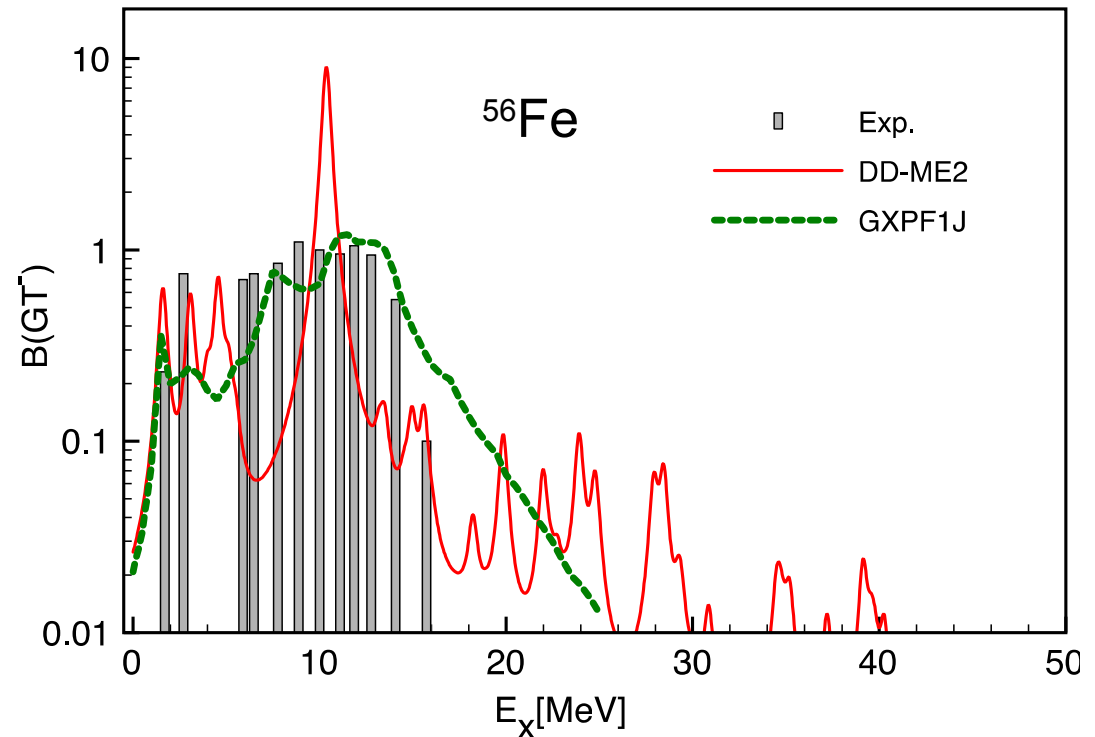
Gamow-Teller (GT) transitions
calculated in two models:

 RQRPA (DD-ME2)

 Shell model (GXPF1J)

T. Suzuki et al.

$$\sigma T_{\mp}$$



- **Shell model** includes important correlations among nuclei, accurately reproduces the experimental GT strength. However, already in medium mass nuclei the model spaces become large, many nuclei and forbidden transitions remain beyond reach.
- **RQRPA** reproduces total GT strength and global properties of transition strength. It allows systematic calculations of high multipole excitations (forbidden transitions), possible extrapolations toward nuclei away from the valley of stability.

LOW-ENERGY NEUTRINO-NUCLEUS PROCESSES



FACT: about 65 million neutrinos pass through your thumbnail every second.

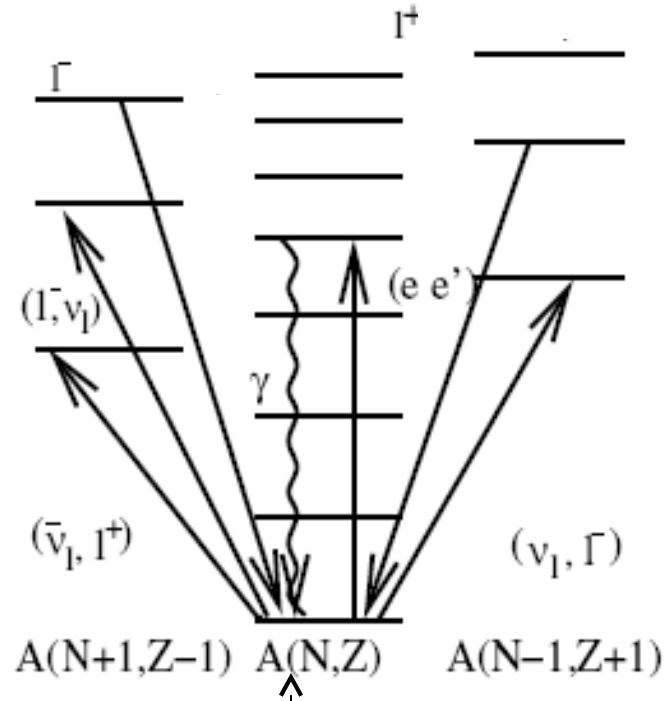
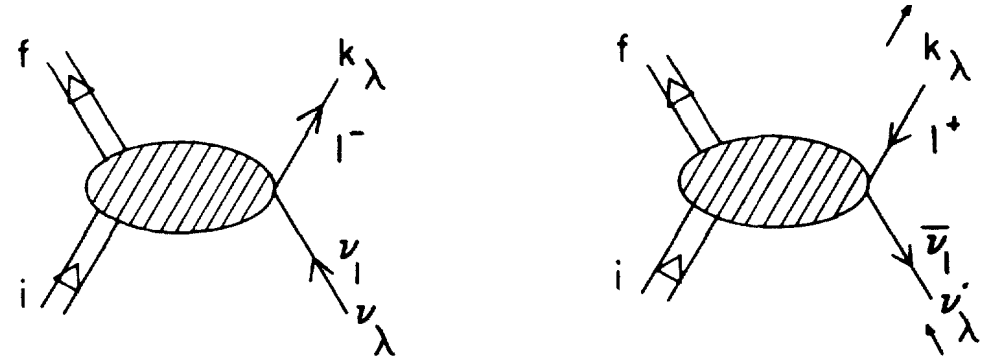
Learn Something
New Every Day.
LSNED.com

Charged-current neutrino-nucleus reactions

$$\nu_l + Z X_N \rightarrow Z+1 X_{N-1}^* + l^-$$

$$\bar{\nu}_l + Z X_N \rightarrow Z-1 X_{N+1}^* + l^+$$

The ground state and excitation properties of nuclei govern the neutrino-nucleus cross sections.



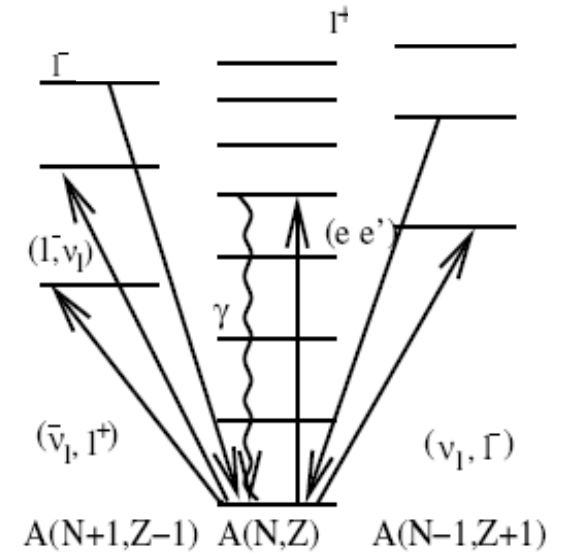
GROUND STATE OF
TARGET NUCLEUS

v-nucleus cross sections

- Weak interaction Hamiltonian + EDF

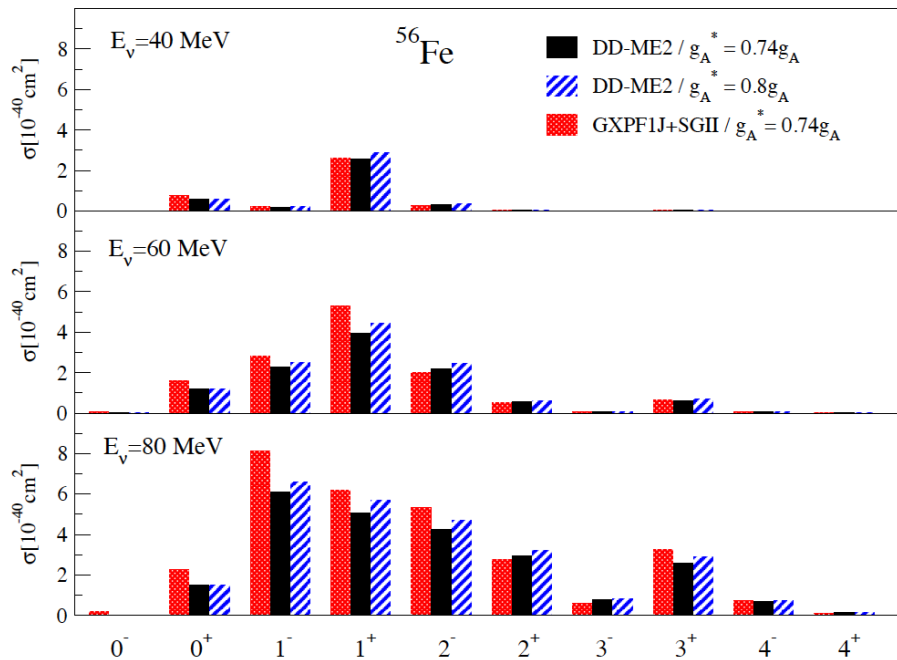
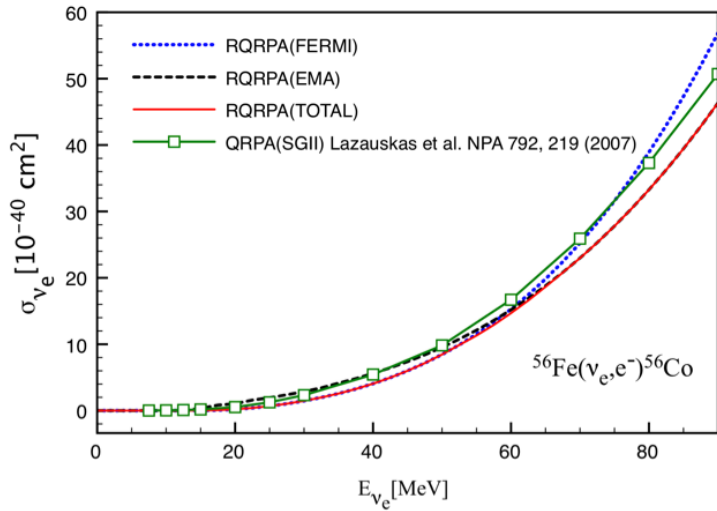
$$\hat{H}_W = -\frac{G}{\sqrt{2}} \int d\mathbf{x} \mathcal{J}^\lambda(\mathbf{x}) j_\lambda(\mathbf{x})$$

$$\begin{aligned} \frac{d\sigma_\nu}{d\Omega} &= \frac{2G_F^2 \cos^2 \theta_c}{\pi} \frac{E_l^2}{2J_i + 1} \\ &\times \left\{ \sum_{J \geq 1} \left\{ [1 - (\hat{\nu} \cdot \hat{\mathbf{q}})(\hat{\mathbf{q}} \cdot \boldsymbol{\beta})] \left[|\langle J_f || \hat{T}_J^{MAG} || J_i \rangle|^2 + |\langle J_f || \hat{T}_J^{EL} || J_i \rangle|^2 \right] \right. \right. \\ &\quad \left. \left. + [\hat{\mathbf{q}}(\hat{\nu} - \boldsymbol{\beta})] 2 \operatorname{Re} \langle J_f || \hat{T}_J^{MAG} || J_i \rangle \langle J_f || \hat{T}_J^{EL} || J_i \rangle^* \right\} \right. \\ &\quad \left. + \sum_{J \geq 0} \left\{ (1 + \hat{\nu} \cdot \boldsymbol{\beta}) |\langle J_f || \hat{\mathcal{M}}_J || J_i \rangle|^2 \right. \right. \\ &\quad \left. \left. + (1 - \hat{\nu} \cdot \boldsymbol{\beta} + 2(\hat{\nu} \cdot \hat{\mathbf{q}})(\hat{\mathbf{q}} \cdot \boldsymbol{\beta})) |\langle J_f || \hat{\mathcal{L}}_J || J_i \rangle|^2 \right. \right. \\ &\quad \left. \left. - [\hat{\mathbf{q}}(\hat{\nu} + \boldsymbol{\beta})] 2 \operatorname{Re} \langle J_f || \hat{\mathcal{L}}_J || J_i \rangle \langle J_f || \hat{\mathcal{M}}_J || J_i \rangle^* \right\} \right\} \end{aligned}$$



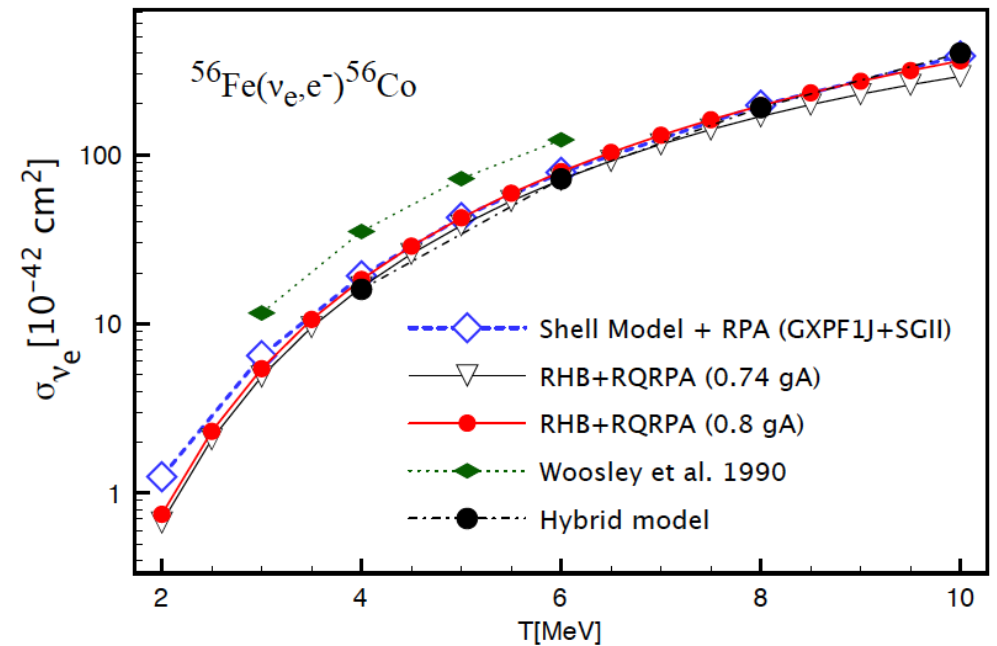
Transition matrix elements are described in a self-consistent way using relativistic Hartree-Bogoliubov model for the initial (ground) state and relativistic quasiparticle random phase approximation for excited states (RHB+RQRPA)

NEUTRINO-NUCLEUS CROSS SECTIONS



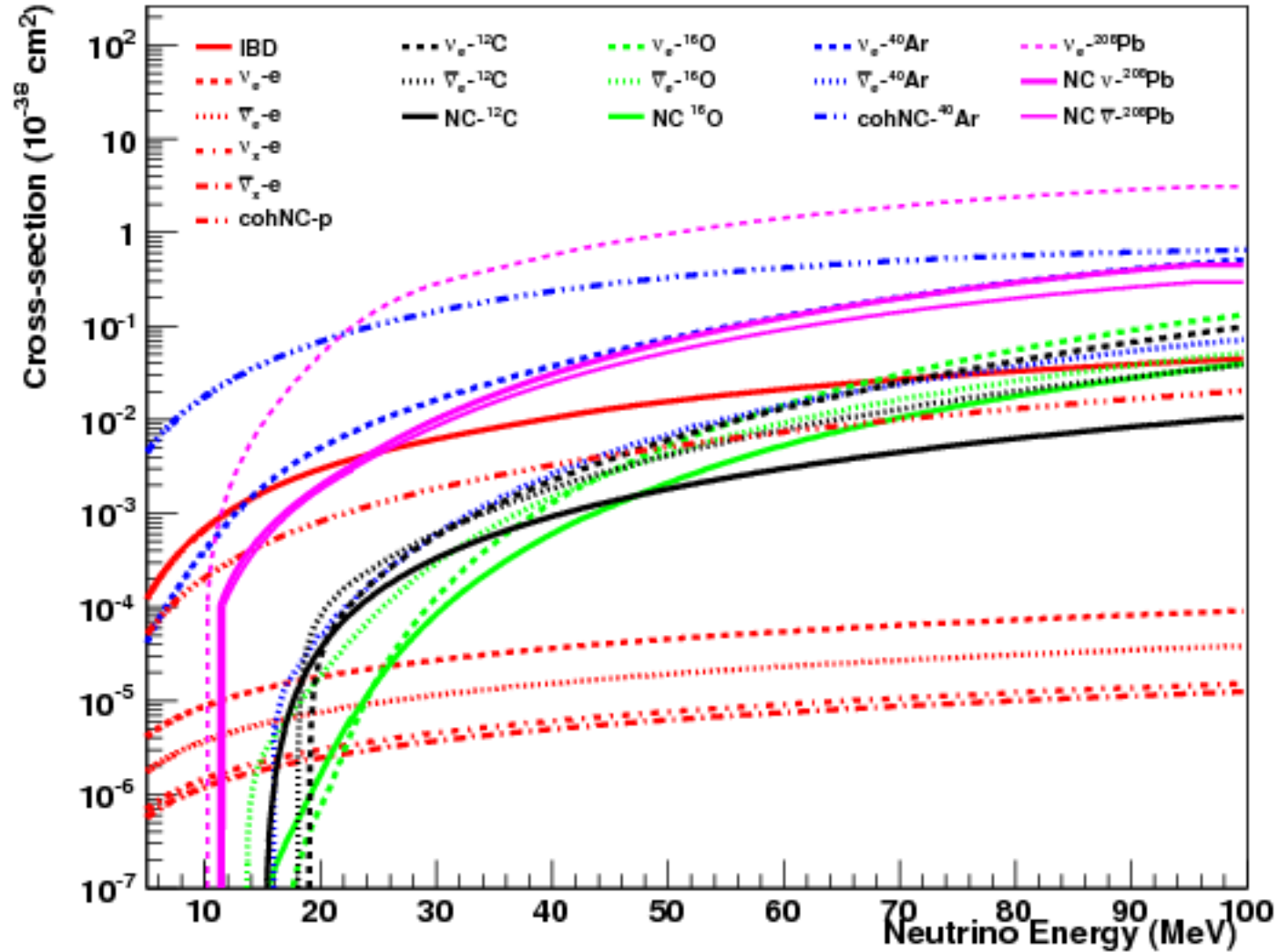
- Cross sections averaged over neutrino flux

$$\langle \sigma_\nu \rangle = \frac{\int dE_\nu \sigma_\nu(E_\nu) f(E_\nu)}{\int dE'_\nu f(E'_\nu)}$$



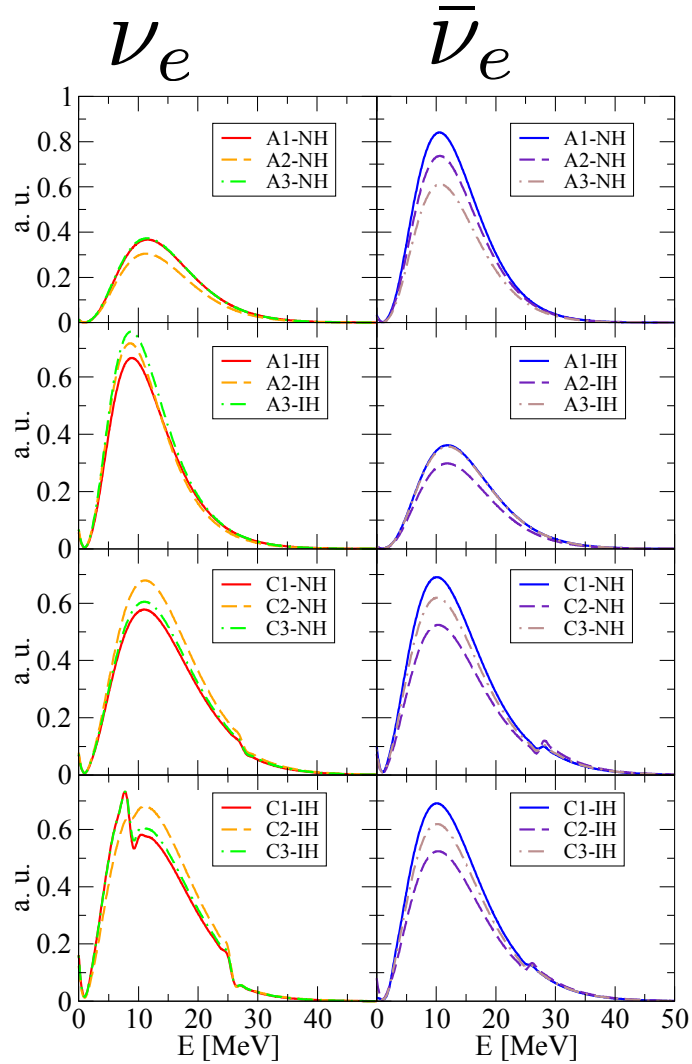
- Multipole decomposition of the neutrino-nucleus cross sections: RNEDF (DD-ME2) vs. shell model + RPA (SGII) (T. Suzuki et al.)

(ANTI)NEUTRINO INDUCED REACTION CROSS SECTIONS



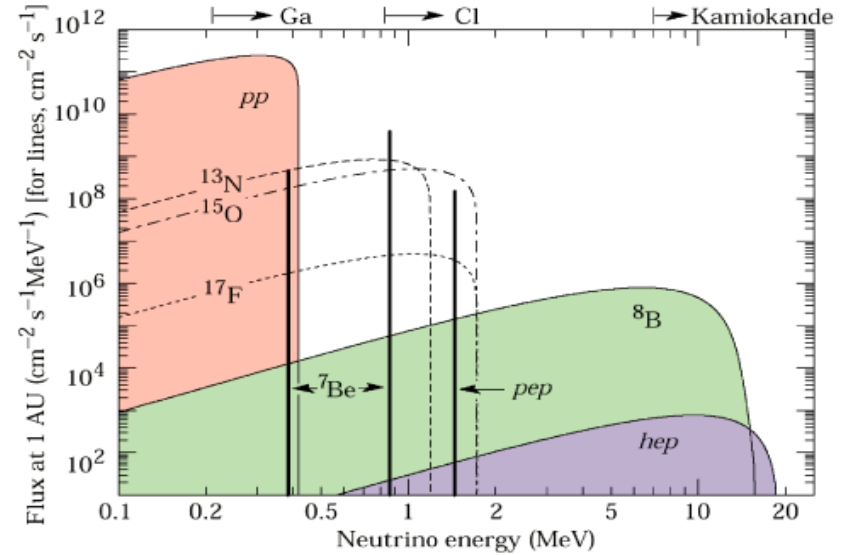
LOW-ENERGY NEUTRINO FLUXES

Supernova neutrinos



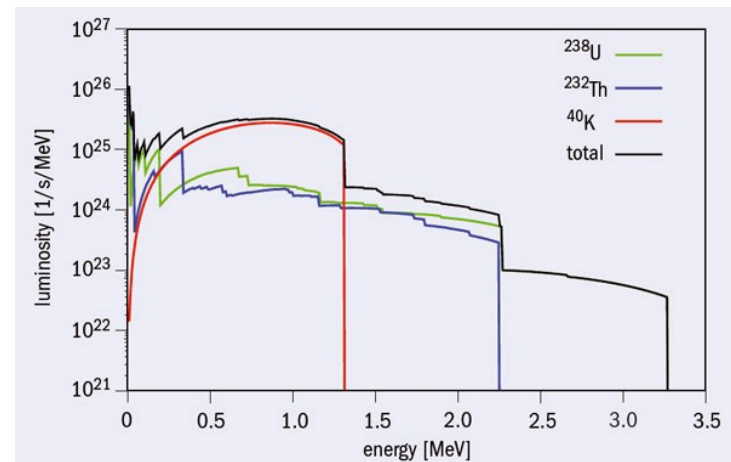
D. Vale, T. Rauscher, N.P., JCAP02, 007 (2016)

Solar neutrinos



Geoneutrinos

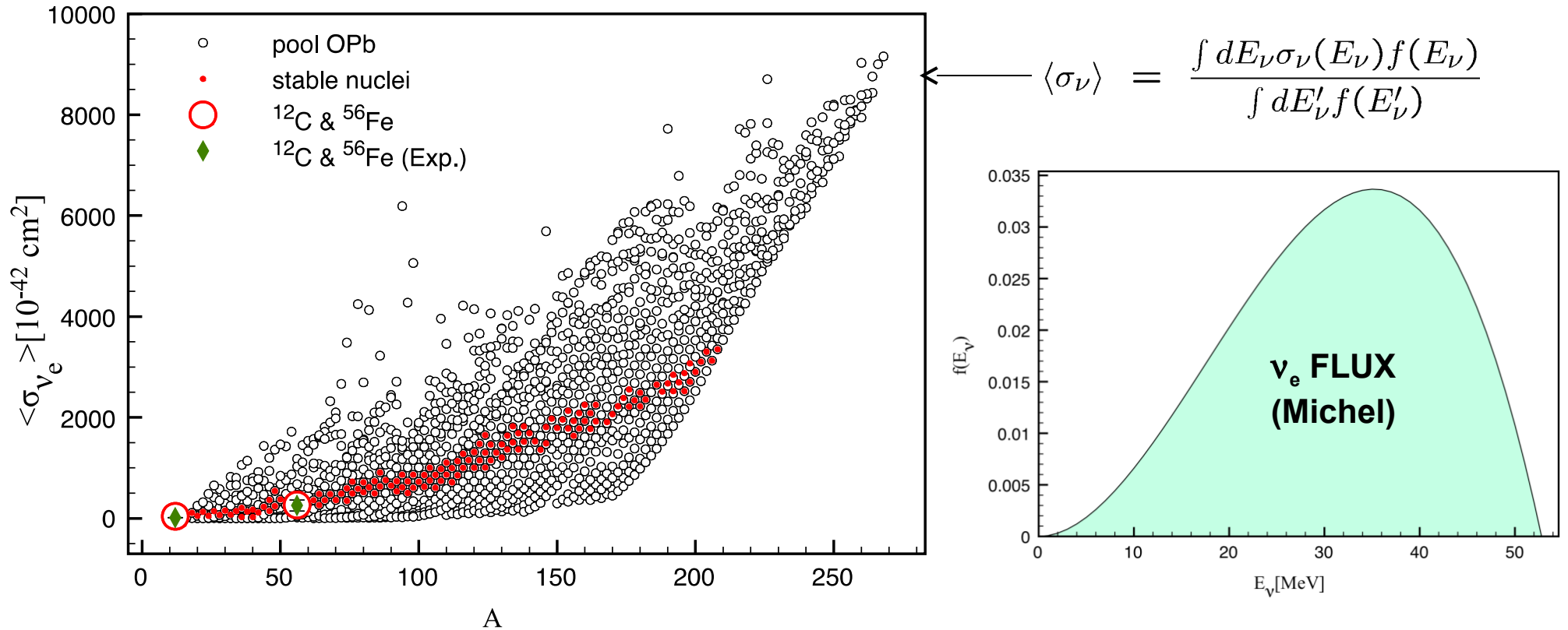
HERON, Brown University (USA)



T. Araki, et al., Nature 436, 499 (2005).

LARGE-SCALE CALCULATIONS OF ν_e -NUCLEUS CROSS SECTIONS

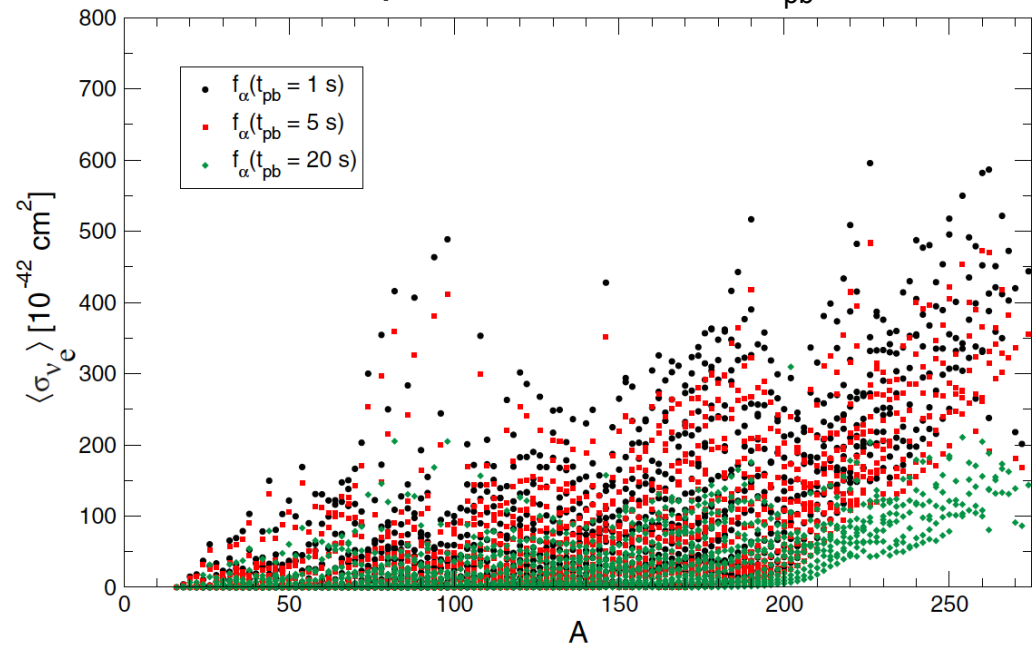
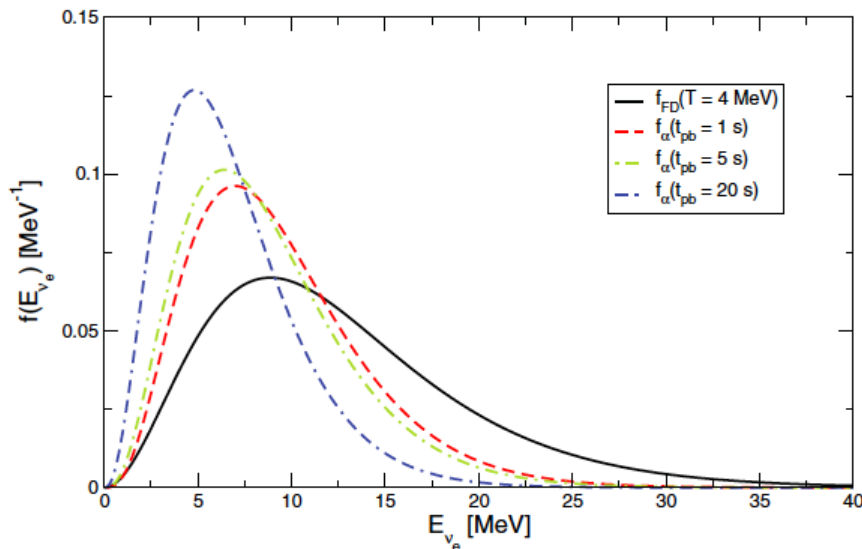
- The cross sections averaged over the neutrino spectrum from muon DAR.



- Exp. data available for ^{12}C and ^{56}Fe
- The cross sections become considerably enhanced in neutron-rich nuclei, while those in neutron-deficient and proton-rich nuclei are small (blocking).

LARGE-SCALE CALCULATIONS OF ν -NUCLEUS CROSS SECTIONS

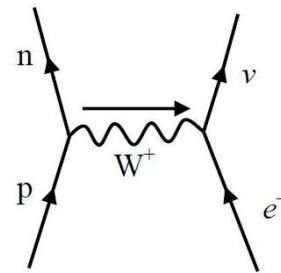
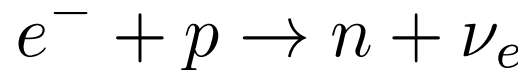
- Neutrino-nucleus cross sections for neutrinos from core collapse supernova simulation
- Supernova model based on general relativistic radiation hydrodynamics and three flavor Boltzmann neutrino transport (Fe core progenitor; $18 M_{\text{solar}}$) (T. Fischer)
- Simulations show continuous decreasing of neutrino luminosities and average energies after the supernova explosion is launched (deleptonization of central protoneutron star)
- Implications for the flux-averaged cross sections at postbounce times $t_{\text{pb}}=1\text{s}, 5\text{s}, 20\text{s}$:



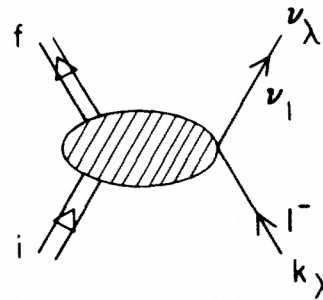
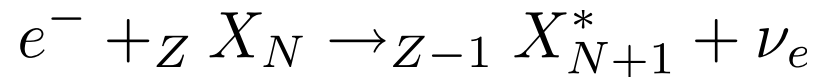
STELLAR ELECTRON CAPTURE

- The core of a massive star at the end of hydrostatic burning is stabilized by electron degeneracy pressure (as long as its mass does not exceed the Chandrasekhar limit)
- Electron capture reduces the number of electrons available for pressure support (in opposition to nuclear beta decay)

Electron capture on protons



Electron capture on nuclei



- Electron capture on iron-group nuclei initiates the gravitational collapse of the core of a massive star, triggering a supernova explosion

STELLAR ELECTRON CAPTURE

- Initial supernova shock location and strength depend on amount of electron capture on nuclei (and protons) during stellar core collapse
- In the early stage of the collapse $\rho \leq 10^{10} \text{gcm}^{-3}$ electron chemical potential is of the order of the nuclear Q value, electron captures are sensitive to the details of Gamow-Teller GT⁺ strength;

$$T \approx 0.3 - 0.8 \text{MeV}$$

$$A < 65$$

- Electron capture also occurs for higher densities and temperatures
- Ⓟ total GT strength and centroid are relevant,
at $\rho \geq 10^{11} \text{gcm}^{-3}$ forbidden transitions should also be taken into account;

$$T \approx 1 \text{MeV}$$

$$A \geq 65$$

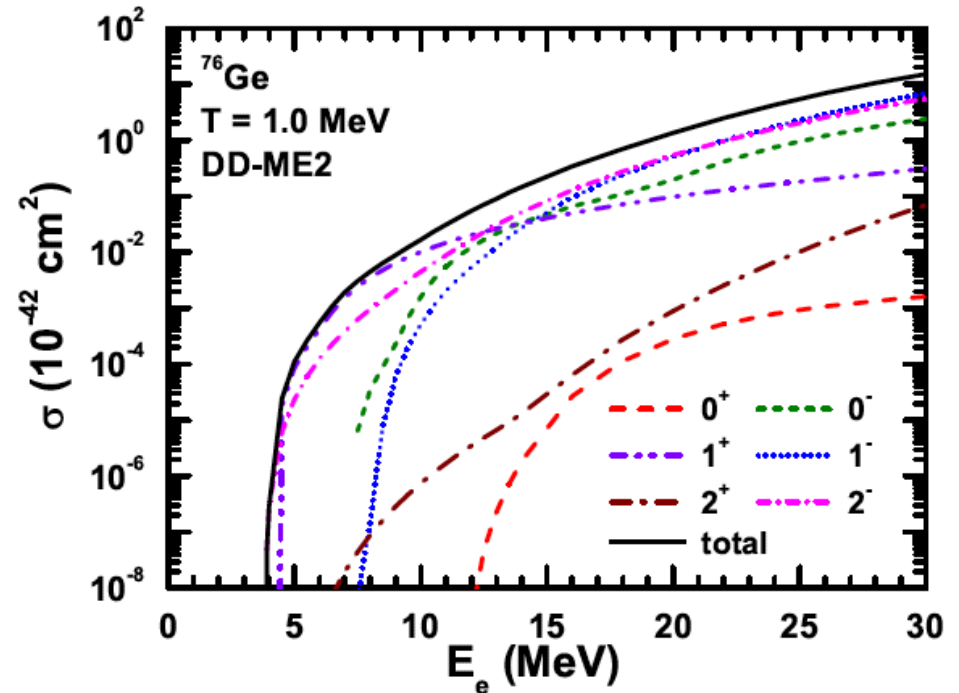
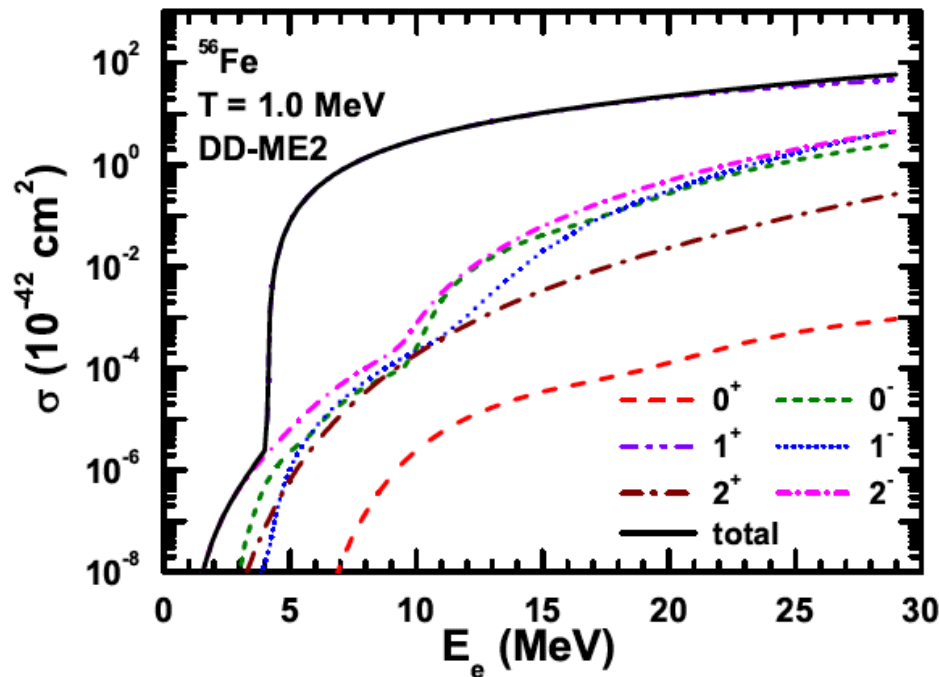
- Shell model, Random Phase Approximation (RPA), QRPA, Hybrid model
- Hartree-Fock+RPA (Skyrme functionals)
- Relativistic mean field + relativistic RPA

} Finite
Temp.

K. Langanke et al., PRL 90, 241102 (2003); A.A. Dzhiyev et al., PRC 81, 015804 (2010)
A. Juodagalvis et al., NPA 848, 454 (2010); N. P., G. Colò, et al., PRC 80, 055801 (2009)
Y. F. Niu, et al., PLB 681, 315 (2009); A. F. Fantina, et al., PRC 86, 035805 (2012).

ELECTRON CAPTURE (EC) CROSS SECTIONS

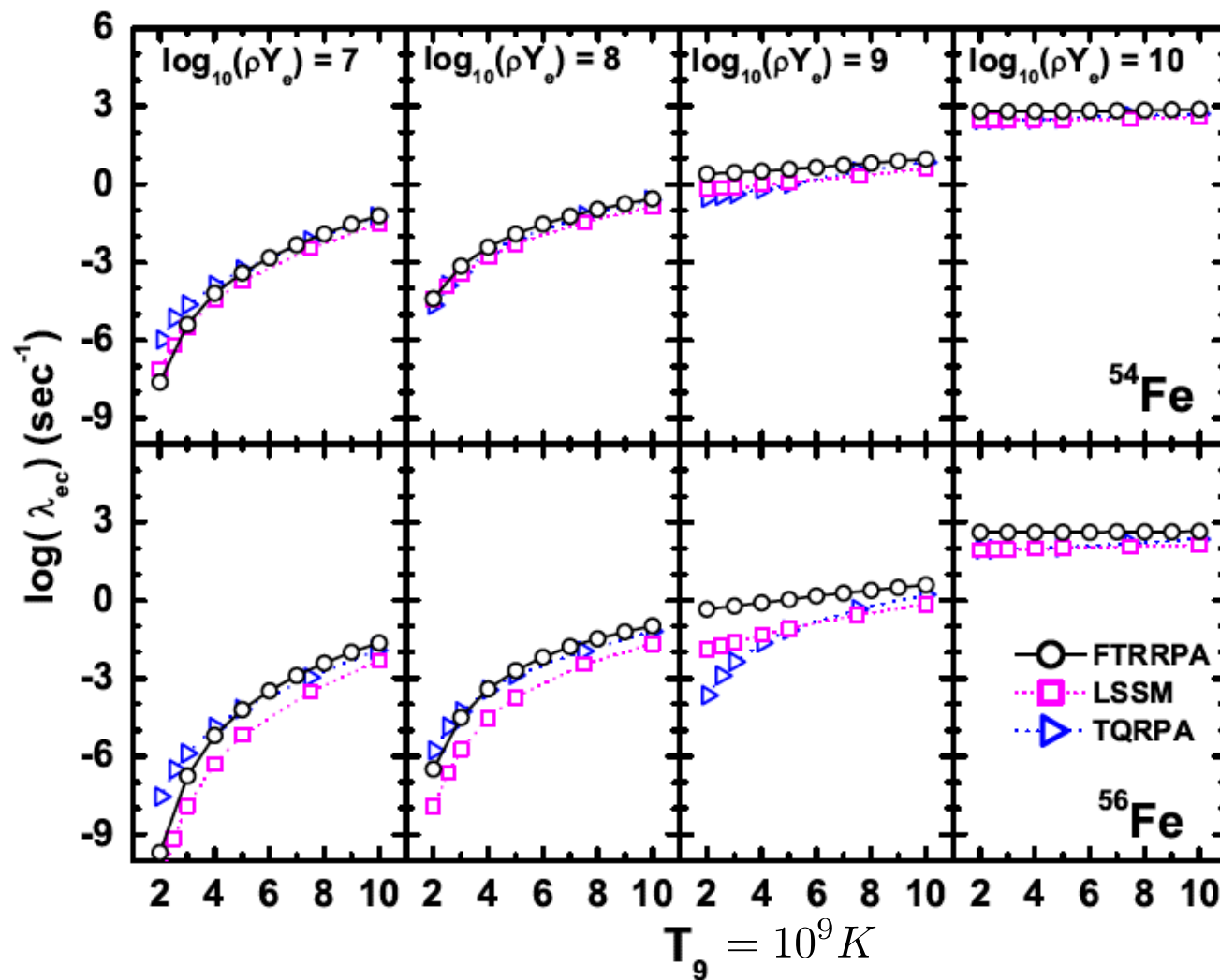
- FTRRPA calculations of the EC cross sections with all multipoles considered
- finite temperature reduces the threshold energy for the electron capture



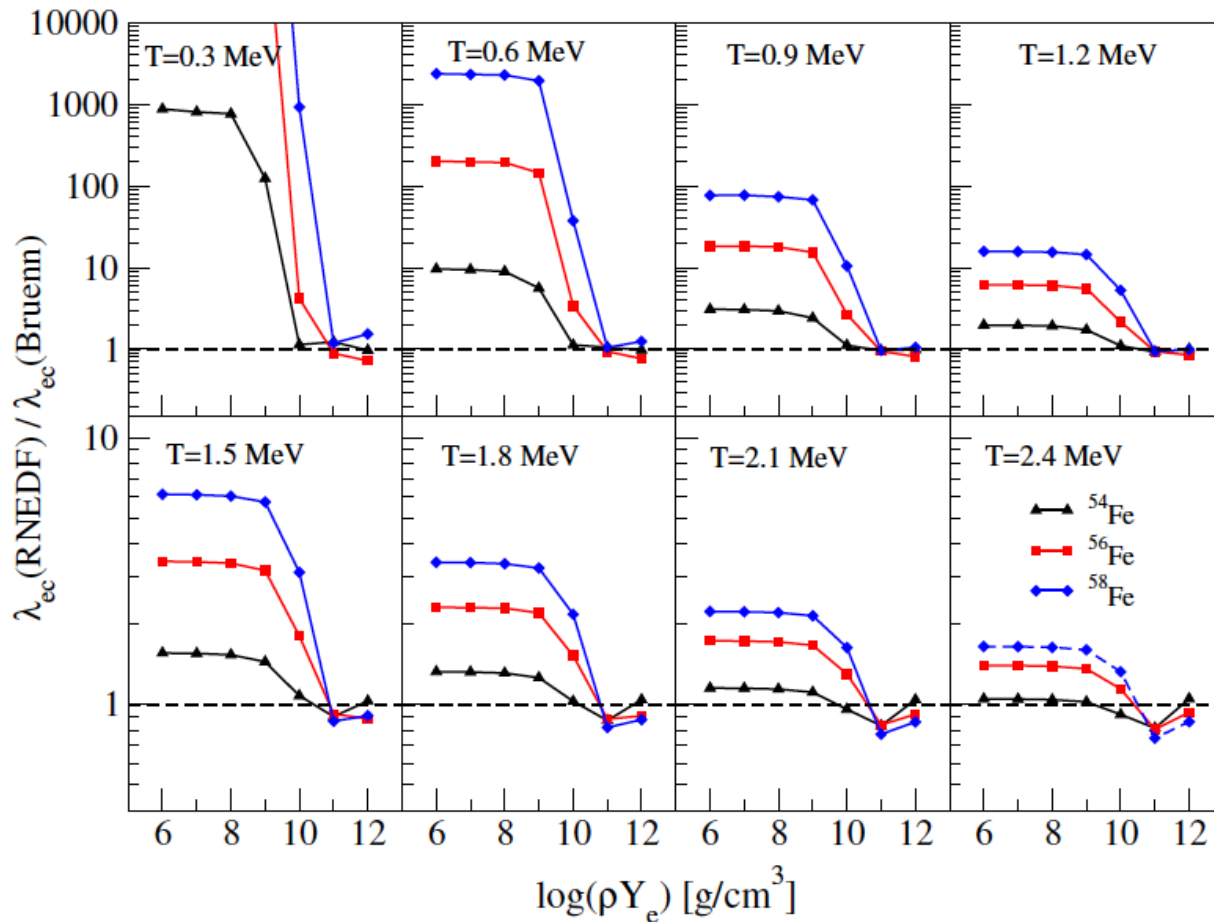
- For ^{56}Fe the electron capture is dominated by the GT+ transitions, while for neutron-rich nuclei (^{76}Ge) forbidden transitions play more prominent role)

STELLAR ELECTRON CAPTURE RATES FOR Fe ISOTOPES

$$\lambda_{ec} = \frac{1}{\pi^2 \hbar^3} \int_{E_e^0}^{\infty} p_e E_e \sigma_{ec}(E_e) f(E_e, \mu_e, T) dE_e$$



STELLAR ELECTRON CAPTURE RATES FOR Fe ISOTOPES



Stellar electron capture rates
for $^{54,56,58}\text{Fe}$:

RNEDF vs. Bruenn rates

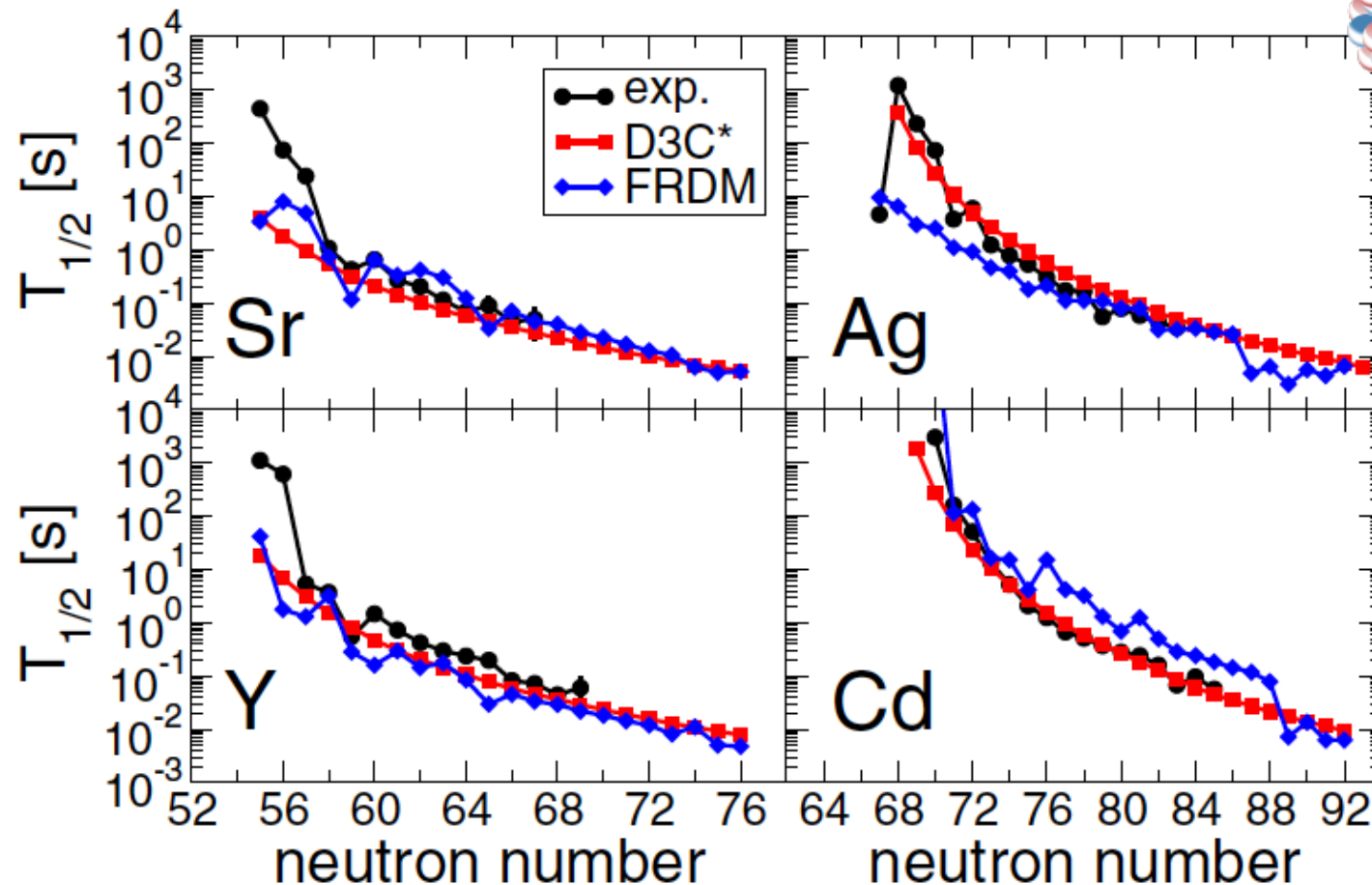
FIG. 7: The ratio between the RNEDF and Bruenn [5] electron capture rates for $^{54,56,58}\text{Fe}$, shown as a function of ρY_e for the range of temperatures $T=0.3, 0.6, \dots, 2.4$ MeV.

N. P. et al. (2016).

S. W. Bruenn, A.J. Supp. 58, 771 (1985).

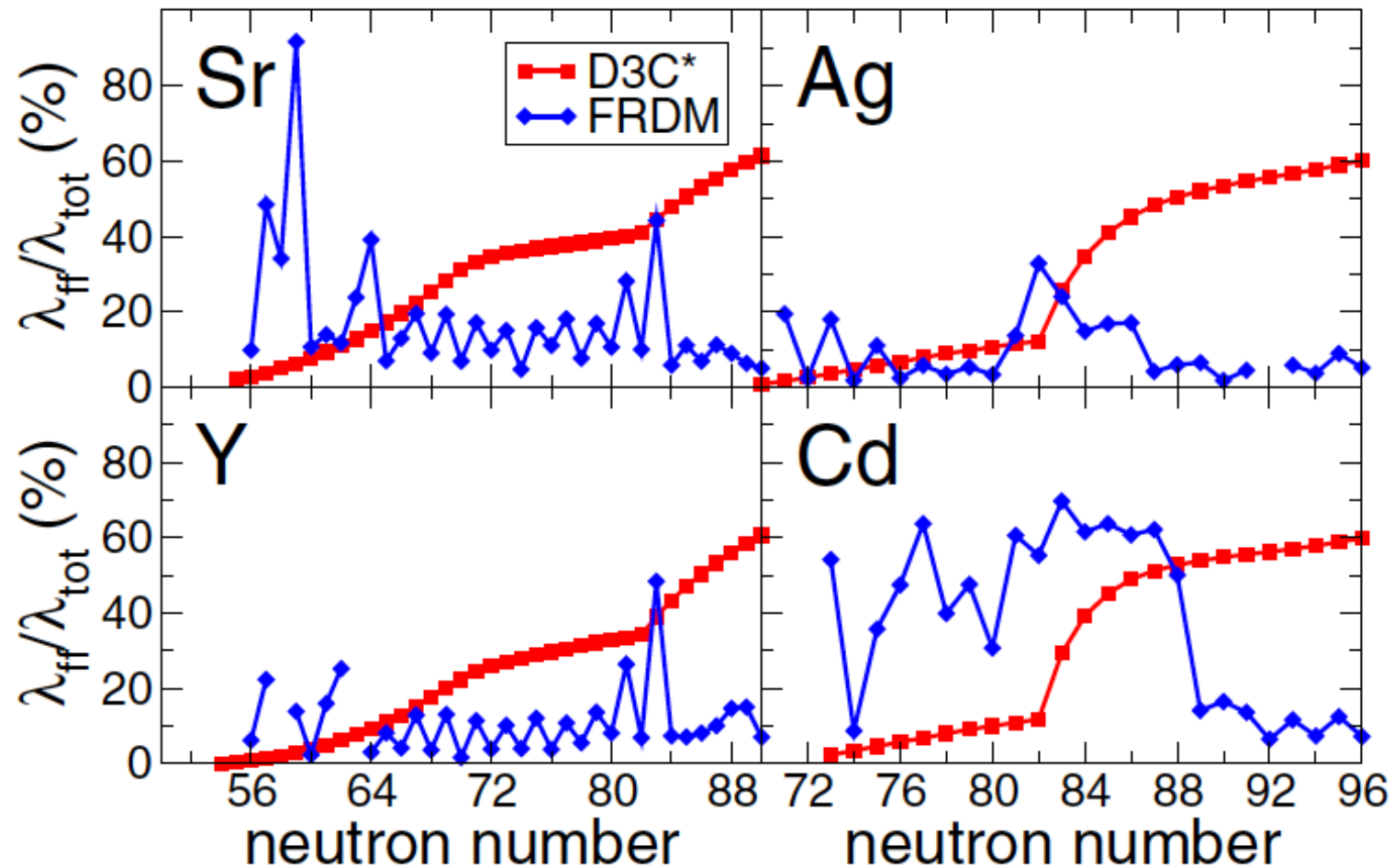
NUCLEAR BETA DECAY

- Nuclear beta decay ${}_Z X_N \rightarrow {}_{Z+1} X_{N-1} + e^- + \bar{\nu}_e$
 - relativistic QRPA calculations including forbidden transitions $L=1$ (T. Marketin et al.)



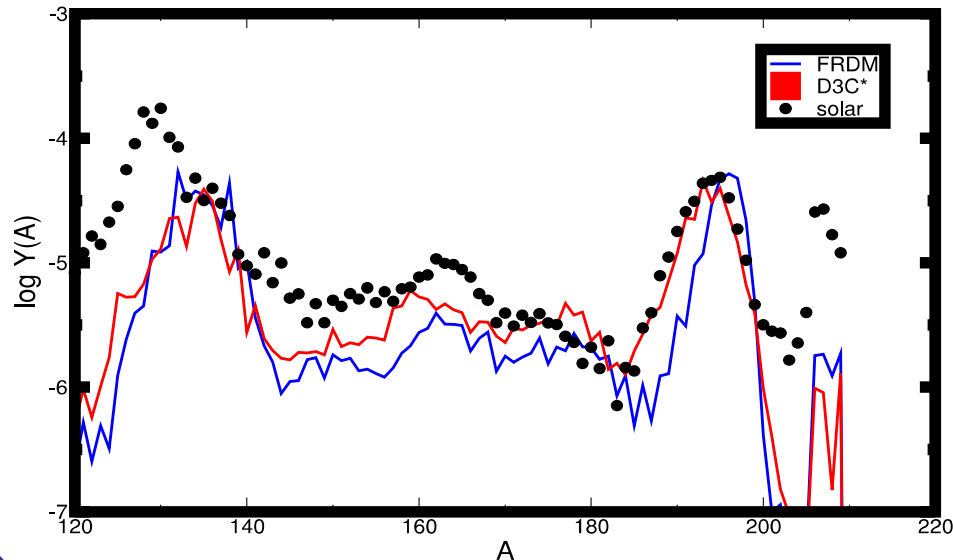
NUCLEAR BETA DECAY

- Contributions from the first forbidden transitions to the beta decay rates

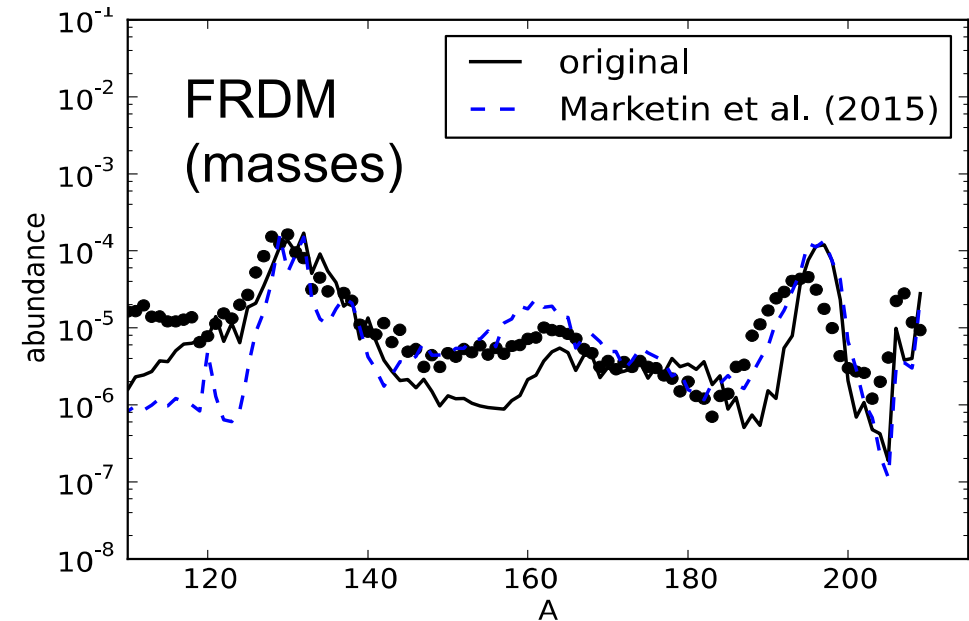
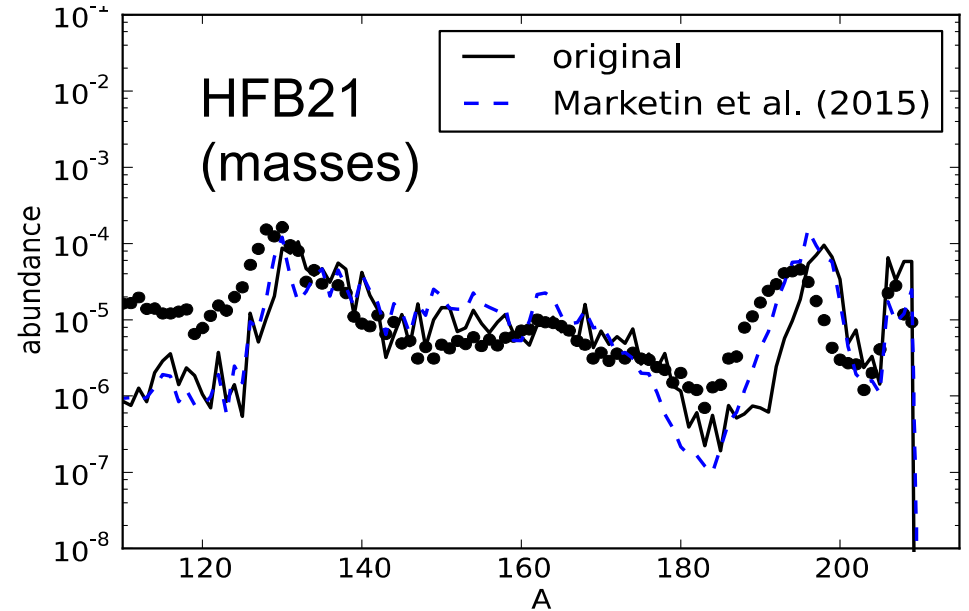


R-PROCES ELEMENT ABUNDANCES

- Beta decay half-lives have a significant impact on the abundance pattern
- third peak is particularly sensitive to the changes
- general results for different conditions



M. Eichler et al., *Astrophys. J.* 808, 30 (2015)



CONCLUDING REMARKS

- consistent nuclear input for astrophysical simulations is still missing – at present time, various results from different models are combined together in supernova and nucleosynthesis simulations
- pairing correlations are mainly neglected in finite temperature frameworks (RPA,RRPA,...) to describe weak interaction processes
- deformation is necessary for complete description of weak interaction processes in some open shell nuclei
- inclusion of complex-configurations in the (Q)RPA will provide detailed structure of transition strength necessary for more reliable description of weak interaction processes